An Assessment of Parameters Describing the Signal Delay in the Neutral Atmosphere Derived from Co-located Instrumentation at the Onsala Space Observatory

Rüdiger Haas, Gunnar Elgered

Abstract We use all VGOS data observed at the Onsala Space Observatory in 2022 to estimate zenith total delays and horizontal gradients with a temporal resolution of 5 min. Corresponding analyses are performed with data from two co-located GNSS stations and a ground-based microwave radiometer. Pairwise comparisons result in correlation coefficients of $\rho > 0.99$ and $\rho > 0.64$ for the zenith total delays and the gradients, respectively. Pairwise offsets are < 1.5 mm for all parameters. The weighted root-mean square differences are on the order of 3–5 mm and 0.5 mm for zenith total delays and the gradients, respectively. This study is encouraging in the sense that is proves that VGOS can resolve signal path delays in the neutral atmosphere with high temporal resolution and a high level of agreement with results derived from independent co-located instrumentation. It also opens up for inter-technique combinations and augmentation in data analysis.

Keywords VGOS · GNSS · WVR · co-location · ZTD · gradients

1 Introduction

The temporal and spatial variation of the signal delay in the neutral atmosphere is one of the major restricting factors for radio-wave-based space-geodetic techniques, such as Very Long Baseline Interferometry (VLBI) and Global Navigation Satellite Systems (GNSS) (Nilsson and Haas, 2010). While the hydrostatic delays can be modeled well based on information of atmospheric pressure and corresponding mapping functions, the so-called wet delays, related to the amount of water vapor, fluctuate rather rapidly. Thus, parameters describing these wet delays are usually estimated in the VLBI and GNSS data analyses, applying appropriate mapping functions. These estimates will also absorb any uncertainties in the a priori hydrostatic delays. Additionally, direction-dependent fluctuations are usually estimated as linear horizontal gradients, including contributions from both hydrostatic and wet parts of the atmosphere. Finally, the analyses of VLBI and GNSS data usually result in time series of zenith total delays (ZTD) and total horizontal gradients in the north and the east directions (NGR, EGR).

Ground-based microwave radiometers, often referred to as water vapor radiometers (WVR), are remote sensing instruments that are sensitive directly to the amount of water vapor in the atmosphere. Thus, by operating a WVR in a so-called sky-mapping mode, it is possible to derive time series of zenith wet delays and horizontal wet gradients. Adding model information based on pressure data to these estimates, also from the WVR time series of ZTD, NGR, and EGR can be derived.

Having access to simultaneously operating co-located instrumentation such as VLBI, GNSS, and WVR provides an opportunity to assess the parameters describing the signal delay in the neutral atmosphere.

In Section 2 we describe the co-located instruments and the corresponding data. Section 3 explains the individual techniques and the specific data analyses that were performed. The resulting time series are compared pairwise in Section 4. Section 5 concludes the paper.

Chalmers University of Technology, Department of Space, Earth and Environment, Onsala Space Observatory, SE-439 92 Onsala, Sweden

2 Data

We study data obtained form the co-located instrumentation for VLBI, GNSS, and WVR at the Onsala Space Observatory (OSO). Figure 1 shows the two VLBI antennas used for observations in the VLBI Global Observing System (VGOS), called O13E and O13W in the following, as well as the two GNSS stations ONSA and ONS1, part of the International GNSS Service (IGS), and the WVR Konrad. All five instruments are co-located within about 500 m and thus can be expected to basically share the same local atmosphere.

A previous study by Haas and Elgered (2023) focused on four VGOS Research & Development (VR) sessions that were observed in 2021 and 2022. These VR sessions were dedicated to achieve as many observations as possible in order to sense the atmosphere at VGOS stations with high temporal resolution. Here we investigated all 42 VGOS sessions in 2022 where the OTT participated. Among them, there were 36 VGOS operational (VO) sessions and six VR sessions. The standard VO sessions do not achieve the high number of observations as the dedicated VR sessions in 2021 and 2022, only about 2,500–3,000 instead of about 5,400–5,800 observations, but nevertheless a reasonably large number that should allow to estimate atmospheric parameters with high temporal resolution. Table 1 provides an overview of the VGOS sessions observed at OSO in 2022.

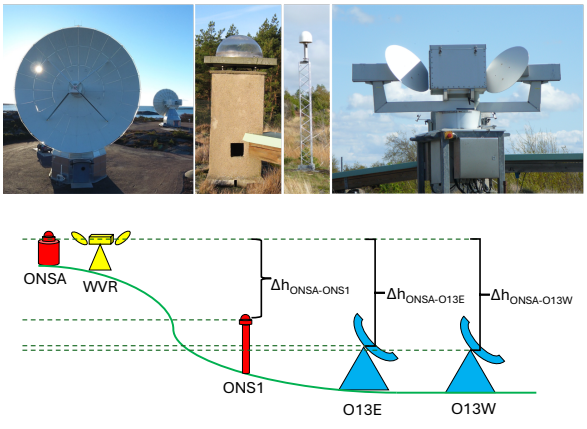

Fig. 1 Top: Co-located instrumentation at the Onsala Space Observatory: The Onsala twin telescopes (left); ONSA and ONS1, two of the GNSS stations (middle); the microwave radiometer (right). Bottom: Sketch showing that the reference points of the instruments are at different heights. The reference points of GNSS station ONSA is at the same height as the one of the microwave radiometer, but it is $\Delta h = 2.1$ m above the one of GNSS station ONS1, and $\Delta h = 6.647$ m and $\Delta h = 6.649$ m above the ones of the VGOS stations O13E and O13W, respectively.

Table 1 Overview of the instrumentation operating at OSO during VGOS sessions in 2022.

Session	Date	O13E	O13W	ONSA	ONS1	WVR
VO2013	2022-01-13	√	√	√	√	√
VR2201	2022-01-20	√	√	√	√	–
VO2027	2022-01-27	√	–	√	√	√
VO2034	2022–02-03	√	–	√	√	√
VO2041	2022–02-10	√	–	√	√	√
VO2048	2022–02-17	√	–	√	√	√
VO2055	2022–02-24	√	–	√	√	√
VO2062	2022–03-03	√	–	√	√	√
VO2069	2022–03-10	√	–	√	√	√
VR2202	2022-03-17	√	–	√	√	√
VO2083	2022–03-24	√	–	√	√	√
VO2090	2022–03-31	√	–	√	√	√
VO2097	2022–04-07	√	–	√	√	√
VO2111	2022–04-21	√	–	√	√	√
VO2118	2022–04-28	√	–	√	√	√
VO2125	2022–05-05	√	–	√	√	√
VO2132	2022–05-12	√	√	√	√	√
VR2203	2022-05-19	–	√	√	√	√
VO2153	2022–06-02	–	√	√	√	√
VO2160	2022–06-09	–	√	√	√	√
VO2167	2022-06-16	√	√	√	√	√
VO2181	2022-06-30	–	√	√	√	√
VO2187	2022-07–06	√	√	√	√	√
VR2204	2022-07-21	√	√	√	√	√
VO2223	2022-08-11	√	√	√	√	√
VO2230	2022-08-18	√	√	√	√	√
VO2237	2022-08-25	√	√	√	√	√
VO2244	2022-09-01	√	√	√	√	√
VO2251	2022-09-08	√	√	√	√	√
VR2205	2022-09-15	√	√	√	√	√
VO2265	2022-09-22	√	√	√	√	√
VO2272	2022-09-29	√	√	√	√	–
VO2279	2022-10-06	√	√	√	√	√
VO2286	2022-10-13	√	√	√	√	√
VO2293	2022-10-20	–	√	√	√	√
VO2299	2022-10-26	√	√	√	√	–
VO2307	2022-11-03	√	√	√	√	√
VR2206	2022-11-09	√	–	√	√	√
VO2321	2022-11-17	√	√	√	√	√
VO2335	2022-12-01	√	√	√	√	√
VO2348	2022-21-21	√	√	√	√	√
VO2363	2022-12-29	√	√	√	√	√

For 22 out of the 42 sessions, both OTT were participating. O13W was not participating between the end of January and early May since its digital backend was sent for repair. O13W did not participate in

VR2206 and O13E did not participate in VO2293 due to lack of disk space. For VO2132, O13W observed just the first 17 hours of the session. For VO2321 and VO2335, O13W missed the first five hours and first 14.5 hours, respectively. The two GNSS stations, ONSA and ONS1, that are part of the IGS, were operating continuously during 2022–2023. The WVR missed three sessions (VR2201, VO2272, VO2299).

3 Data Analysis

The VGOS data were analyzed with a least-squares approach using the ASCOT software (Artz et al., 2016), following the analysis strategy recommended for the ITRF2020 processing (Gipson, 2020). The VMF3 mapping functions were applied (Landskron and Böhm, 2018) with a minimum elevation cutoff of 5°. Very loose constraints of 21.6 cm/h for ZWD and 2.16 cm/h for NGR and EGR were applied to estimate these signal delay parameters with a temporal resolution of 5 min. The final zenith total delays (ZTD) resulted in adding the estimated ZWD and the a priori zenith hydrostatic delays (ZHD) that were modeled using the local pressure recorded in the VLBI logfiles.

Multi-GNSS data (i.e., GPS, GLONASS, Galileo) were analyzed with the Kalman-filter based software GipsyX (Bertiger et al., 2020) using precise point positioning (PPP) (Zumberge et al., 1997). The VMF1 mapping functions (Boehm et al., 2006) were used with a minimum elevation cutoff of 7°. The Kalman-filter analysis used a 5-min temporal resolution and loose variance constraints: 1 cm^2/h for ZWD and 3 mm^2/h for NGR and EGR. The final ZTD resulted in adding the estimated ZWD and the a priori ZHD.

To analyze the WVR data we used an in-house software (Elgered et al., 2019). It is based on an unconstrained least-squares analysis and applies a sky-mapping strategy with an elevation cut-off of 25°. The temporal resolution of the derived ZWD and gradients is 5 min. Periods with rain and individual observations through dense water clouds (equivalent zenith liquid water content > 0.7 mm) were deleted. Since the WVR is exclusively sensitive to wet delays and wet gradients, ZHD calculated based on in-situ pressure data, were added to the WVR-derived ZWD, and hydrostatic gradients, based on the VMF products, were added to the WVR-derived wet gradient parameters.

Table 2 Median formal errors of ZTD, NGR, and EGR derived from the analysis of VLBI, GNSS, and WVR data.

	σ-ZTD (mm)	σ-NGR (mm)	σ-EGR (mm)
VGOS	1.65	0.31	0.31
GNSS	1.50	0.28	0.30
WVR	0.12	0.06	0.06

Since the reference points of the individual instruments are at different heights, see Figure 1, corresponding corrections were applied to refer all ZTD to a common reference height (Rothacher et al., 2011). The common reference height was chosen to be the height of the GNSS station ONSA. Table 2 gives an overview of the median formal errors of the ZTD, NGR, and EGR parameters derived from the individual analyses.

As an example, Figure 2 depicts time series of ZTD, NGR, and EGR derived from all five techniques for one VGOS session in the summer of 2022. During this 24-hour period, the ZTD showed a rather large variation of about 130 mm, which was sensed nicely by all five techniques. Small-scale fluctuations in NGR and EGR were also sensed with all five techniques. From the gradient time series is becomes evident that the GNSS analysis used looser constraints than the VLBI analysis. However, since both techniques use different analysis strategies, least-squares for VLBI and Kalman-filter for GNSS, it is difficult to compare the constraints. Both VLBI and GNSS results agree well with the independent WVR results.

4 Comparisons

The resulting signal delay parameters, ZTD and gradients, of all three techniques were compared pairwise. We chose the ONSA GNSS station and the O13E VGOS telescope for these comparisons because they acquired the largest amount of data during the 42 experiments. Doing so, there were 10,440 data points for the conmparison of GNSS and VGOS, 5,879 data points for the comparison of VGOS and WVR, and 6,431 data points for the comparison of GNSS and WVR. Figure 3 depicts the pairwise correlations between the three techniques for all 42 experiments in 2022, as well as offsets and weighted root mean square (WRMS) differences. The ZTD are highly correlated with correlation coefficients above 0.99, while, as expected, the NGR and EGR parameters show less correlation but still all above 0.63.

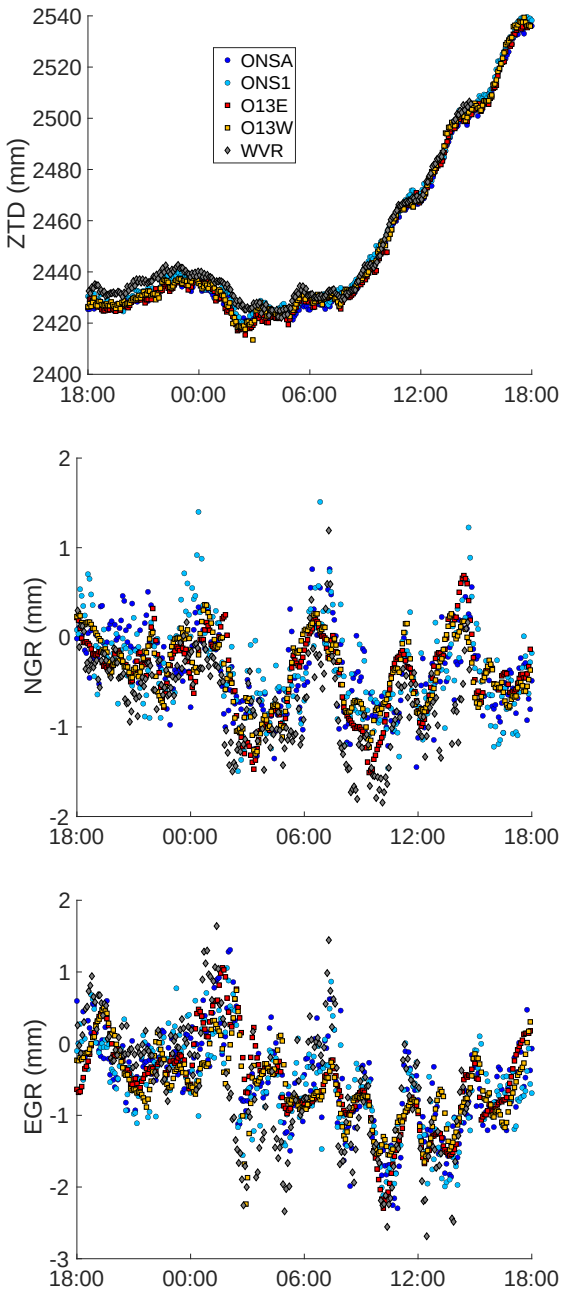

Fig. 2 Time series of ZTD derived for VO2167 on 16/17 June 2022. The ZTD variation is about 130 mm during this 24-hour period.

The pairwise offsets are < 1.5 mm for the ZTD, and not statistically significant for the gradient parameters. The WRMS differences are on the order of 3–5 mm and < 0.5 mm for ZTD and gradients, respectively.

5 Conclusions

Our comparison of signal path delay parameters derived from co-located instrumentation at OSO during 42 VGOS sessions in 2022 shows good agreement among the investigated techniques. We conclude that the comparison of VGOS and GNSS results with the corresponding results from a co-located and independent WVR are meaningful for a temporal resolution as high as 5 min. Small-scale variations in ZTD, NGR, and EGR are clearly detectable by all three techniques.

The ZTD agree pairwise with correlation coefficients $\rho > 0.99$. Pairwise offsets of ZTD are < 1.5 mm, and the weighted root mean square (WRMS) differences are on the order of 3–5 mm.

As expected, the agreement for horizontal total gradient parameters is worse. However, even here, pairwise correlation coefficients of $\rho > 0.63$ are achieved. The gradient offsets are insignificant and the WRMS differences are about 0.5 mm.

In general, this high level of agreement between co-located and independent techniques is encouraging. Our conclusion is that VGOS data analysis should operationally determine signal delay parameters with high-temporal resolution. It opens also up for inter-technique combinations as well as inter-technique augmentation in the data analysis.

References

Artz T et al. (2016) ivg::ascot: Development of a new vlbi software package. In: Behrend, Baver, Armstrong (eds) *IVS 2016 General Meeting Proceedings*, **NASA/CP-2016-219016**, 217–221, https://ivscc.gsfc.nasa.gov/publications/gm2016/045_artz_etal.pdf

Bertiger W et al. (2002) GipsyX/RTGx, a new tool set for space geodetic operations and research. *ASR*, 66(3), 469–489, doi:10.1016/j.asr.2020.04.015

Boehm J, Werl B, Schuh H (2006) Troposphere mapping functions for GPS and very long baseline interferometry from European Centre for Medium-Range Weather Forecasts operational analysis data. *J. Geophys. Res.*, 111, B02406, doi:10.1029/2005JB003629

Elgered G et al. (2019) On the information content in linear horizontal delay gradients estimated from space geodesy observations, *AMT*, 12, 3805–3823, doi:10.5194/amt-12-3805-2019

Gipson J (2020) IVS Checklist for ITRF2020. https://ivscc.gsfc.nasa.gov/IVS_AC/ITRF2020/ITRF2020_checklist_v2020Jan13.pdf

Haas R, Elgered G (2023) Atmospheric parameters derived from VGOS sessions observed with the Onsala twin telescopes. In: Haas, Schroth, Neidhardt (eds) *Proc. 26th European VLBI for*

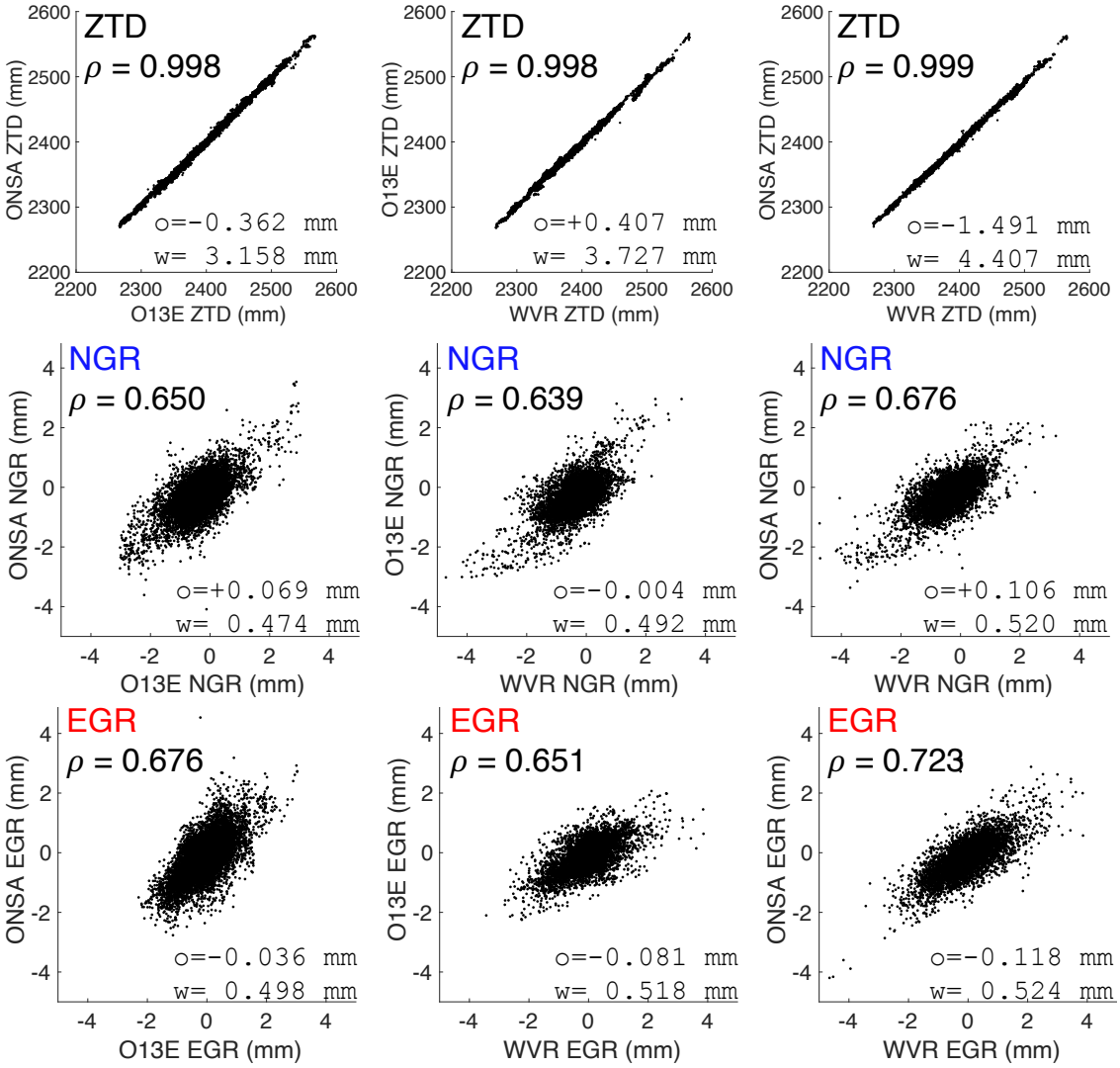

Fig. 3 Pairwise correlations of ZTD (top row), NGR (middle row), and EGR (bottom row) for GNSS/ONSA, VGOS/O13E, and WVR. There are 10,440 data points each for GNSS/ONSA vs. VGOS/O13E (left column), 5,879 data points each for VGOS/O13E vs. WVR (middle column), and 6,431 data points each for GNSS/ONSA vs. WVR (right column). Besides the correlation coefficients (ρ), also the pairwise offsets (o) and weighted root mean square differences (w) are given. Note that, because the pairwise comparisons do not use the identical time periods, they cannot be compared to each other in terms of accuracy.

Geodesy and Astrometry (EVGA) working meeting, 76–80, doi:10.14459/2023md1730292

Landskron D, Böhm J (2018) VMF3/GPT3: refined discrete and empirical troposphere mapping functions. *J Geod*, 92, 349–360, doi:10.1007/s00190-017-1066-2

Nilsson T, Haas R (2010) Impact of atmospheric turbulence on geodetic very long baseline interferometry. *JGR* 115(B3), doi:10.1029/2009JB006579

Ning T, Elgered G (2021) High-temporal-resolution wet delay gradients estimated from multi-GNSS and microwave radiometer observations. *AMT*, 14, 5593–5605, doi:10.5194/amt-14-5593-2021

Rothacher M et al. (2011) GGOS-D: homogeneous reprocessing and rigorous combination of space geodetic observations. *J Geod*, 85(10):679–705, doi:10.1007/s0019 0-011-0475-x

re3data.org: VMF Data Server; editing status 2020-12-14; re3data.org - Registry of Research Data Repositories, doi:10.17616/R3RD2H

Zumberge J F et al. (1997) Precise Point Positioning for the efficient and robust analysis of GPS data from large networks. *JGR*, 102(B3), 5005–5017, doi:10.1029/96JB03860